Calibration of a Chromatic Confocal Microscope for Measuring a Colored Specimen

Qing Yu
Kun Zhang
Ruilan Zhou
Changcai Cui
Fang Cheng
 Shiwei Fu
Ruifang Ye
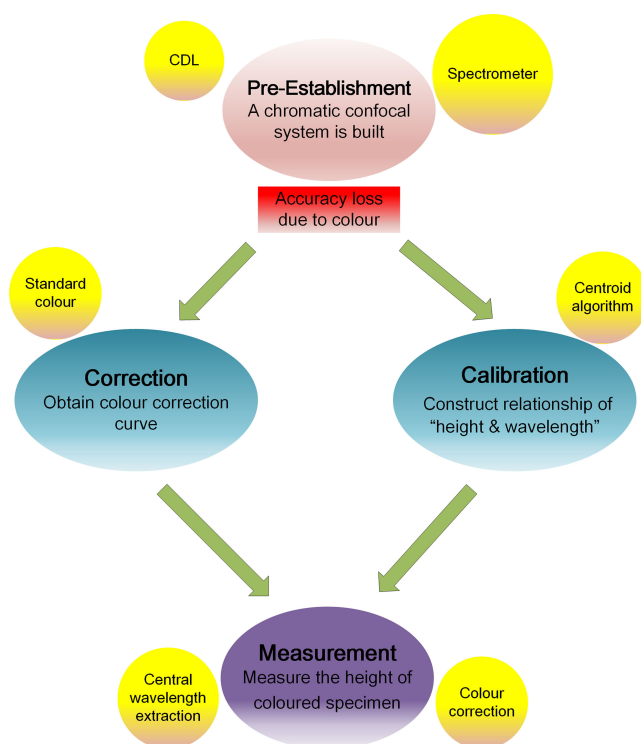
Calibration of a Chromatic Confocal Microscope for Measuring a Colored Specimen

Qing Yu [ID],[1] **Kun Zhang** [ID],[1] **Ruilan Zhou,**[1] **Changcai Cui,**[2] **Fang Cheng,**[1] **Shiwei Fu,**[1] **and Ruifang Ye**[1]

[1]College of Mechanical Engineering and Automation, Huaqiao University, Xiamen 361021, China
[2]Institute of Manufacturing Technology, Huaqiao University, Xiamen 361021, China

Abstract: In this paper, a color correction method is proposed to improve measurement accuracy for chromatic confocal microscopy (CCM) when measuring a colored specimen. Characteristic curve shifting due to selective reflection from color surfaces was analyzed based on a laboratory CCM system developed by the authors' team. Theoretically, when the color of the targeted surface is different from that represented by the central wavelength of the light source, the characteristic curve of CCM would have a notable deviation from that of an achromatic surface. In this study, this conclusion was verified through both simulation and experiments. Using a set of standard color calibration pieces, a color correction method was proposed accordingly to quantify the characteristic curve shifting. To validate the proposed method, a laser scanning confocal microscope Carl Zeiss LSM700 was used as the referencing system. Experimental data showed that with the color correction method, measurement errors can be controlled within 10 nm. Compared with the measurement without color correction, the measurement accuracy is significantly improved.

Index Terms: Chromatic confocal microscopy, colour specimen, spectral information, characteristic curve shifting, colour correction curve.

1. Introduction

The confocal technique has become a powerful measurement method in various microscopic imaging applications because of its capabilities of superior resolution, rejection of scattered light and depth discrimination [1]–[4]. In a classic confocal microscopy system, vertical scanning is required to generate a Depth Response Curve (DRC), the peak of which specifies the height of the current measurement points. To perform fast areal measurements, high-speed lateral scanning techniques have been maturing in the recent decade, such as Nipkow disk [5], micro lens array (MLA) [6], and digital micromirror device (DMD) [7]. However, height measurement based on vertical scanning on each measurement point is still the efficiency bottleneck for most conventional, monochrome confocal systems.
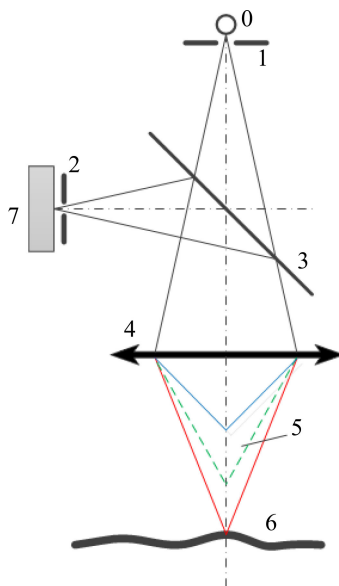
Fig. 1. Schematic diagrams of the principle of the chromatic confocal system. 0. Polychromatic light source, 1. Pinhole 1, 2. Pinhole 2, 3. Beam splitter, 4. Chromatic dispersion lens, 5. Chromatic dispersion region, 6. Specimen, 7. Spectrometer.

To perform faster height measurements, the chromatic confocal microscopy (CCM) technique was proposed and has evolved [8]–[10] in recent years. Instead of physical scanning in the vertical direction, a CCM system takes use of a polychromatic light source to emit lights with different wavelengths, which are dispersed in the axial direction to form a series of focal points. The light with a certain wavelength that focuses onto the specimen indicates the height of the current measurement point. Many efforts have been made towards performance improvements for CCM, such as the structural design of CCM systems, the development of chromatic dispersion devices, the algorithm of chromatic confocal measurement, and the strategies on accuracy improvement. Garzón [11] proposed a mathematic measurement model to address the challenge of nonlinearity caused by the dispersive optics. Hillenbrand [12] presented a novel mathematical function IPSF (Intensity Point Spread Function) to reshape the characteristic curve of a CCM system. Using this method, the measurement repeatability and computation efficiency can be improved. Liu [13] proposed a dispersive objective configuration, in which the negative and positive lens groups could generate the linear axial chromatic dispersion with specified focal power distribution. Chen [8] integrated the DMD technique into a CCM system to eliminate the necessity of both vertical and lateral mechanical scanning structures. Lyda [14] combined a spectral interferometer with small measuring range and a chromatic confocal method with low accuracy to establish a chromatic-confocal spectral interferometry (CCSI), which increased the robustness of the system. Taphanel [15] used a monochrome line scan camera with six rows as the detector and acquired high speed capability.

However, the compensation of the measurement errors caused by specimen colour remains challenging work. According to the CCM principle, when a light beam is reflected by the specimen surface, the height information of the specimen is carried by the spectrum and is decoded by a spectrometer. Therefore, the colour of a specimen will inevitably affect the measurement accuracy due to the characteristic curve shifting effect. This challenge is addressed in this paper, and a colour correction method is proposed accordingly.

2. Principle of the Chromatic Confocal Method

Figure 1 shows the optical structure of a CCM system. The polychromatic light source has a continuous spectrum that consists of different wavelengths. Using the chromatic dispersion lens,

the confocal points with maximum light intensity in object space are distributed along the optical axis. This wavelength distribution could be expressed as a function of $\lambda(z)$, where z is the axial position; the output result of light intensity in object space is given by [16]:

$$I(u) = \left[\frac{\sin(u/4)}{u/4}\right]^4 \tag{1}$$

where $u = \frac{2\pi}{\lambda(z)} z \sin^2 \alpha$.

As shown in Eq. (1), according to the variable $\lambda(z)$, there are infinite intensity peaks in the distribution curve of CCM in theory. This "multi-peaks" characteristic enables a CCM system to perform height measurement without mechanical scanning. Therefore, height can be measured by decoding the spectral information of the reflected light.

3. Influence of the Colour Specimen

If the specimen has an achromatic (e.g., grey or metallic colour) surface that has a consistent reflection/absorption ratio for light of different wavelengths, then CCM is a reliable measurement technology. However, when the specimen has a chromatic colour, it will reflect the illumination light selectively and accordingly cause spectral shifting.

To concentrate on the influence of the specimen colour, the intensity spread function of the incidence light (illumination light) and the colour function of specimen surface are defined as I (A, λ, z) and I' (x, y, A', λ'), respectively, where A is the amplitude, and λ is the wavelength. Because it is difficult to express I (A, λ, z) in the form of a continuous equation, a discrete expression is used in this paper:

$$I(A, \lambda, z) = (I_1(A_1, \lambda_1, z_1), I_2(A_2, \lambda_2, z_2), \ldots, I_n(A_n, \lambda_n, z_n)) \tag{2}$$

where I_1, I_2..., I_n are the intensity distribution functions at different wavelengths within the wavelength range of visible light.

When the light beam is reflected by the specimen surface, the intensity distribution function I_{ref} (A, λ, z) will be the convolution of the intensity spread function of the incident light I (A, λ, z) and the colour function of the specimen surface I' (x, y, A', λ'); thus, the intensity distribution function is given by

$$I_{ref}(A, \lambda, z) = I(A, \lambda, z) * I'(x, y) = (I_1(A_1, \lambda_1, z_1), I_2(A_2, \lambda_2, z_2), \ldots, I_n(A_n, \lambda_n, z_n)) * I'(x, y, A', \lambda') \tag{3}$$

Assuming the specimen has a consistent colour over the whole measurement area, the colour function can be simplified as a constant. As a result, I' (x, y, A', λ') is considered as location-independent and can be expressed as I' (A', λ'). Accordingly, Eq. (3) is simplified as:

$$I_{ref}(A, \lambda, z) = (I_1(A_1, \lambda_1, z_1), I_2(A_2, \lambda_2, z_2), \ldots, I_n(A_n, \lambda_n, z_n)) * I'(A', \lambda') \tag{4}$$

As shown in Fig. 1, when measurement point is at a certain height z_i, only one chromatic component with the wavelength λ_i passes through the pinhole and forms the maximum intensity on the spectrometer, while the remaining chromatic components are significantly weakened by the pinhole. Ignoring the off-focus components, the output intensity distribution can be expressed as

$$I_{ref}(A, \lambda, z) = I_i(A_i, \lambda_i, z_i) * I'(A', \lambda') \tag{5}$$

where I_i (A_i, λ_i, z_i) is the intensity function with a maximum intensity of z_i.

In Eq. (5), it is not difficult to find that λ in I_{ref} (A, λ, z) is the convolution of λ_i and λ'. Because the surface has a consistent colour, i.e., λ' is constant, it can be concluded that the intensity distribution curve will shift a distance along the z-position axis. The evolution of the intensity curve, curve of cyan light is taken for example, is shown in Fig. 2.

However, the wavelength shifting distance and direction have not been determined. In further research, it was found that the shifting distance and direction are strongly correlated with the
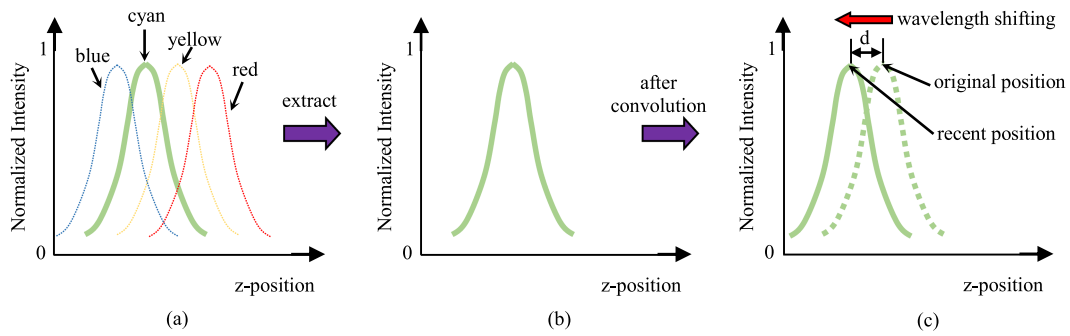
Fig. 2. Evolution of the intensity distribution curve in Eq. (5), with cyan light as an example. (a) Wavelength discretization of the light beam over the sample surface. (b) Original intensity-position curve of cyan light. (c) Intensity-position curve shifting *d* of the of the cyan light after convolution.
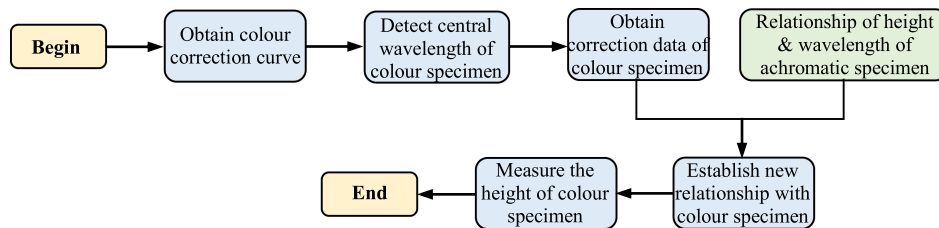

Fig. 3. Flow chart of the height measurement of a coloured specimen.

spectral colour. As shown in Fig. 2, cyan light is taken as an example. After convolution with the surface colour function, the intensity peak shifts left by a distance of d; and the value of d is determined by the difference between λ_0, the central wavelength of the light source, and λ', the wavelength is represented by the specimen colour. Therefore, the wavelength shifting distance can be expressed as

$$d = k \cdot (\lambda_0 - \lambda') \tag{6}$$

where k is the coefficient of wavelength shifting.

In Eq. (6), the value and sign of d indicate the shifting distance and direction, respectively. If the sign is positive, then the intensity distribution curve shifts leftwards; otherwise, it shifts rightwards.

4. Simulation and Experiments

Before measuring colour specimens, the baseline was built by modelling the relationship between z-position (height) in object space and the wavelength of the light source through vertically scanning an achromatic specimen. Next, the colours of a set of colour specimens were determined by measuring the central wavelengths of the reflected light for each specimen. With the information of known colour, the shifting values of height-wavelength curves were calibrated. The calibration results were used to compensate the measurement errors caused by the specimen colour. The whole process can be expressed by the flow chart shown in Fig. 3.

An experimental CCM platform was built by the authors' team, as shown in Fig. 4. The components used in this setup are listed in Table 1.

In this experimental platform, the CDL, which was designed in previous research [17], is able to form a linear dispersion range of the focal points. An achromatic reflector was used to determine the central wavelength of the halogen lamp. Based on the centroid algorithm [18], the central wavelength of the halogen lamp was calculated to be 608 nm.
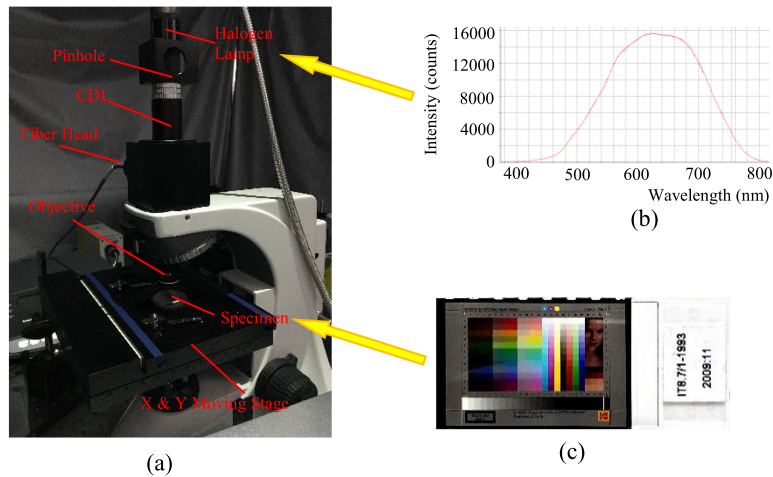
Fig. 4. Drawing of the experiment platform. (a) Experimental platform based on the principle of the chromatic confocal microscope (the objective is 10×, which's NA is 0.3). (b) The spectral distribution of the halogen lamp, as detected by the spectrometer of HR2000+, of which the central wavelength is approximately 608 nm, as calculated by the centroid algorithm. (c) Kodak Q-60 colour input target.

TABLE 1

List of Components Used in the Experimental CCM Platform

Components	Producer	Function
Halogen lamp	Moritex	Polychromatic light source
Chromatic dispersion lens	Self-built	Produce chromatic dispersion
Q-60 colour input target	Kodak	Standard colour plate
100μm pinhole	Edmund Optics	filter
HR2000+	Ocean Optics	Spectrometer

In Fig. 4, an inductance micrometre Tesa TT80 is used to record the z-displacement the stage. When the stage moves along z-direction step by step, the spectrometer captures the spectral data from an achromatic specimen frame by frame. The spectral data are calculated by the centroid algorithm, and a series of wavelengths data can be obtained. Next, the data of z-displacements and wavelengths are plotted as the 'height-wavelength' curve. The simulation results of three height-wavelength curves of the experimental CCM are shown in Fig. 5.

After being reflected by the chromatic coloured specimen, this characteristic curve will shift along the wavelength direction. As discussed in Section 3 and shown in Fig. 5, when the central wavelength of the specimen surface is longer than the calculated central wavelength of light source, the curve will move rightwards, as represented by the curve 'γ'; otherwise, it will move leftwards, as represented by the curve 'α'.

The standard colour plates of red, green, cyan, magenta and yellow were selected from KODAK Q-60 to verify the characteristic curve shifting in the experiment platform. As a baseline, a group
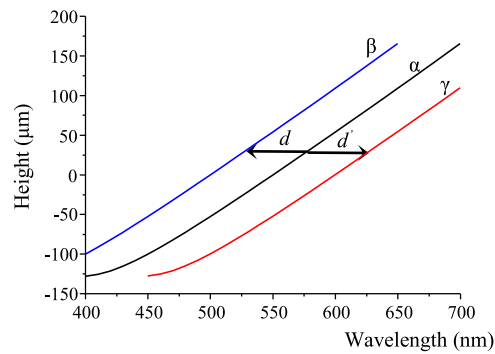
Fig. 5. Simulation of the 'height-wavelength' curve. α: the simulation result under the condition of an achromatic specimen. β, γ: the shifting result when measuring a coloured specimen.
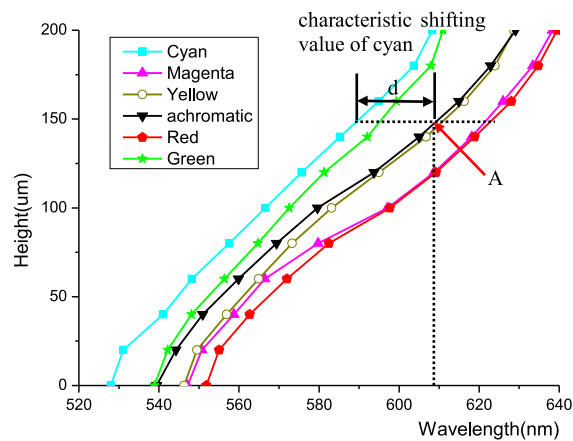

Fig. 6. Experimental results of characteristic curve shifting.

of data collected with an achromatic specimen was also obtained. The shifting values of their height-wavelength curves are shown in Fig. 6.

Compared with the simulation results in Fig. 5, the curves in Fig. 6 plotted by the actual measurement results show shorter wavelength range and lower linearity. The root causes are from the actual components used in this study: the workable wavelength range the halogen lamp used in this system covers only 540–640 nm, instead of the full spectrum of visible light; and the CDL has inherent nonlinearity that deformed the characteristic curve. This paper presents the colour correction method which focuses on the shifting of the characteristic curves. Therefore the nonlinearity won't significantly affect the performance of the proposed method.

It is shown that the height-wavelength curve of the central wavelength of the light source (black curve in Fig. 6) is very close to that of the yellow light. Therefore, a yellow specimen shows very insignificant shifting, which is similar to the behavior of an achromatic surface. When the specimen has a red or magenta surface that selectively reflects long-wavelength light, the height-wavelength curve moves rightwards. In contrast, for a green surface that selectively reflects short-wavelength light, the height-wavelength curve moves leftwards.

As discussed above, the central wavelength of the light source is 608 nm. The point A in Fig. 6 indicates the height of an achromatic surface determined by the central wavelength of the light source. At this height, each deviation value d is taken as the character curve shifting value, as listed in Table 2.

TABLE 2

Characteristic Curve Shifting Values of Different Specimen Colours From KODAK Q-60 (nm)

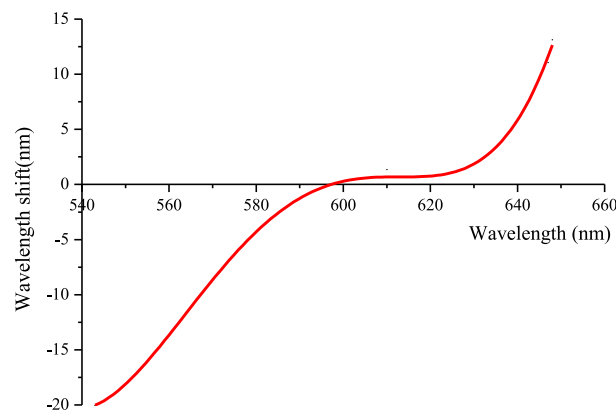|	Calculated central wavelength from Fig. 6	Characteristic curve shifting	True central wavelength of every colour
Red	621.1	13.1	648
Magenta	619.1	11.1	647
Yellow	609.4	1.4	610
Green	592.4	-15.6	556
Cyan	588.0	-20.0	543
Achromatic	608.0	0	608

Fig. 7. Colour correction curve.

Using 4-order polynomial fitting, the shifting values of the characteristic curve are illustrated in Fig. 7. In practical measurements, when the specimen colour is known, these shifting values can be used to compensate measurement errors caused by the specimen colour.

Fig. 7 shows a nonlinear deviation curve. When the difference of specimen colour is close to the central wavelength of the light source, the difference being smaller than 20 nm, then the characteristic curve shifting is insignificant. When the colour difference increases, the amount of characteristic curve shifting increases significantly.

To verify the error compensation method through colour correction curve, three metal plates with different colours were tested. Primarily, the colours of these metal plates were detected by the HR2000+ spectrometer, and their central wavelengths were calculated. To avoid environmental disturbance, the experiments were conducted in a dark room with well-controlled temperature. The wavelength results and characteristic curve shifting values (from Fig. 7) are listed in Table 3.

These correction values were used to recalculate the height of the colour metal plates, and the measured results are shown in Table 4, in which their true heights were measured by laser scanning confocal microscope Carl Zeiss LSM 700.

TABLE 3

Experimental Results: The Central Wavelengths of Three Types of Colour Metal Plates (nm)

	Test 1	Test 2	Test 3	Test 4	Test 5	Result	Characteristic curve shifting values
Colour 1	644.3	644.5	645.0	644.9	644.8	644.7	9.5
Colour 2	635.9	635.0	635.0	635.5	635.2	635.3	3.5
Colour 3	586.8	587.1	587.0	587.3	587.2	587.1	-2.0

TABLE 4

Measured Results for Heights of the Three Types of Colour Metal Plates (μm)

	Heights measured by CCM		Heights measured by LSM700
	Before colour correction	After colour correction	
Colour 1	24	166	160
Colour 2	117	170	176
Colour 3	217	185	190

The comparison shows that without the colour correction, the measurement errors are unacceptable, especially when the specimen colour is significantly different from the central wavelength light from the light source. After colour correction, the measurement accuracy is improved to the nanometre level.

5. Conclusion

For achromatic specimen measurement, chromatic confocal microscopy is able to achieve high measurement accuracy when the height-wavelength relationship is properly calibrated. However, the colour of the specimen surface will cause a shift of the characteristic curve, resulting in significant measurement errors. In this paper, the impact of the specimen colour was theoretically analysed. The colour correction curve was established, and a chromatic confocal measurement process for a coloured specimen was proposed, based on a CCM system developed by the authors' team. To validate the proposed method presented in this paper, the heights of three types of colour metal plates were measured. The experimental results indicated that after error compensation using the proposed method, the measurement results were very close to those from a laser confocal system. Therefore, it can be concluded that the proposed method is a useful tool to effectively improve measurement accuracy for CCM technology, especially when measuring a coloured specimen.

References

[1] L. Qiu, Y. Xiao, and W. Zhao, "Laser differential confocal radius measurement method for the cylindrical surfaces," *Opt. Exp.*, vol. 24, no. 11, 2016, Art. no. 12012.

[2] S. Stach *et al.*, "Assessment of possibilities of ceramic biomaterial fracture surface reconstruction using laser confocal microscopy and long working distance objective lenses," *Microsc. Res. Techn.*, vol. 79, no. 5, pp. 385–392, 2016.

[3] P. Gao and G. U. Nienhaus, "Confocal laser scanning microscopy with spatiotemporal structured illumination," *Opt. Lett.*, vol. 41, no. 6, pp. 1193–1196, 2016.

[4] Ch. Chen *et al.*, "Offset-noises Interactions on peak extraction in confocal microscopy e," *Appl. Opt.*, vol. 57, no. 22, pp. 6516–6526, 2018.

[5] T. Azuma and T. Kim, "Super-resolution spinning-disk confocal microscopy using optical photon reassignment," *Opt. Exp.*, vol. 23, no. 11, pp. 15003–15011, 2015.

[6] J. Lim, M. Jung, and C. Joo, "Development of micro-objective lens array for large field-of-view multi-optical probe confocal microscopy," *J. Micromechanics Microeng.*, vol. 23, no. 6, 2013, Art. no 065028.

[7] Y. Zhang, S. Strube, and G. Molnar, "Parallel large-range scanning confocal microscope based on a digital micromirror device," *Optik*, vol. 124, no. 13, pp. 1585–1588, 2013.

[8] L. C. Chen, Y. W. Chang, and H. W. Li, "Full-field chromatic confocal surface profilometry employing digital micromirror device correspondence for minimizing lateral cross talks," *Opt. Eng.*, vol. 51, no. 8, 2012, Art. no. 081507.

[9] T. Kim, S. H. Kim, and D. Do, "Chromatic confocal microscopy with a novel wavelength detection method using transmittance," *Opt. Exp.*, vol. 21, no. 5, pp. 6286–6294, 2013.

[10] P. Andersson and B. Hemming, "Determination of wear volumes by chromatic confocal measurements during twin-disc tests with cast iron and steel," *Wear*, no. 338, pp. 95–104, 2015.

[11] J. Garzón, J. Meneses, and G. Tribillon, "Chromatic confocal microscopy by means of continuum light generated through a standard single-mode fibre," *J. Opt. A: Pure Appl. Opt.*, vol. 6, no. 6, pp. 544–548, 2004.

[12] M. Hillenbrand, B. Mitschunas, and B. Brill, "Spectral characteristics of chromatic confocal imaging systems," *Appl. Opt.*, vol. 53, no. 32, pp. 7634–7642, 2014.

[13] Q. Liu, C. W. Yang, and D. C. Yuan, "Design of linear dispersive objective for chromatic confocal microscope," *Opt. Precis. Eng.*, vol. 21, no. 10, pp. 2473–2479, 2013.

[14] W. Lyda, M. Gronle, and D. Fleischle, "Advantages of chromatic-confocal spectral interferometry in comparison to chromatic confocal microscopy," *Meas. Sci. Technol.*, vol. 23, no. 5, pp. 54009–54015, 2012.

[15] M. Taphanel, "Multiplex acquisition approach for high speed 3D measurements with a chromatic confocal microscope," *Proc. SPIE*, vol. 9525, 2015, Art no. 95250Y.

[16] T. M. Wilson, *Confocal Microscopy*. New York, NY, USA: Academic Press, 1990.

[17] Ch. C. Cui *et al.*, "Design of adjustable dispersive objective lens for chromatic confocal system," *Opt. Precis. Eng.*, vol. 25, no. 4, pp. 343–351, 2017.

[18] D. Luo, C. Kuang, and X. Liu, "Fiber-based chromatic confocal microscope with Gaussian fitting method," *Opt. Laser Technol.*, vol. 44, no. 4, pp. 788–793, 2012.